Fermilab

Particle Physics Division
Mechanical Department Engineering Note

Number: MD-ENG-082 Date: 6/28/2005

Project Internal Reference:

Project: BTeV Pixel

Title: Prototyping and Testing BTeV Pixel TPG Substrates

Author(s): C. M. Lei

Reviewer(s): Jim Fast, Simon Kwan

Key Words: BTeV, Pixel, TPG, substrate

Abstract Summary: The BTeV experiment proposed at the Fermilab Tevatron will have a pixel detector system. Since this detector will be located inside the ultra high vacuum of the Tevatron, one of the design goals of its cooling system is to have a joint-free system to avoid any possibility of leakage. The mechanism of heat removal is based on conduction. This is achieved by using highly thermally conductive thermal pyrolytic graphite (TPG) as the substrate, where the pixel modules will be placed. However, a large temperature distribution across the pixel sensor area might be built up, and its corresponding stresses and displacements have to be checked to make sure that these would not be excessive. We have put together substrate prototypes and studied the thermal displacement. The prototyping of these substrates, in addition, provided an opportunity to practice the substrate assembly.

Applicable Codes:

Prototyping and Testing BTeV Pixel TPG Substrates

Engineering Note 082

C. M. Lei
PPD/MD

Fermi National Accelerator Laboratory
P. O. Box 500, Batavia, Illinois 60510

Abstract

The BTeV experiment proposed at the Fermilab Tevatron will have a pixel detector system. Since this detector will be located inside the ultra high vacuum of the Tevatron, one of the design goals of its cooling system is to have a joint-free system to avoid any possibility of leakage. The mechanism of heat removal is based on conduction. This is achieved by using highly thermally conductive thermal pyrolytic graphite (TPG) as the substrate, where the pixel modules will be placed. However, a large temperature distribution across the pixel sensor area might be built up, and its corresponding stresses and displacements have to be checked to make sure that these would not be excessive. We have put together substrate prototypes and studied the thermal displacement. The prototyping of these substrates, in addition, provided an opportunity to practice the substrate assembly.

I. Introduction

The BTeV detector, which is proposed to be installed at the C zero interaction region at FermiLab, consisted of a series of detector elements covering the whole tracking volume. At the core of this region, is the pixel detector which composed of 60 pixel planes each with its silicon modules being glued onto the TPG substrates. These silicon modules will be aligned vertically and horizontally so that the X- and Y-measuring planes are formed. These modules are glued to the TPG substrate, and the heat generated from these modules, will be conducted away to the ends at which the substrates will be clamped to the cold blocks. This layout is shown in Figure 1 in which a station consisting of the X-view and Y-view measuring substrates is shown.

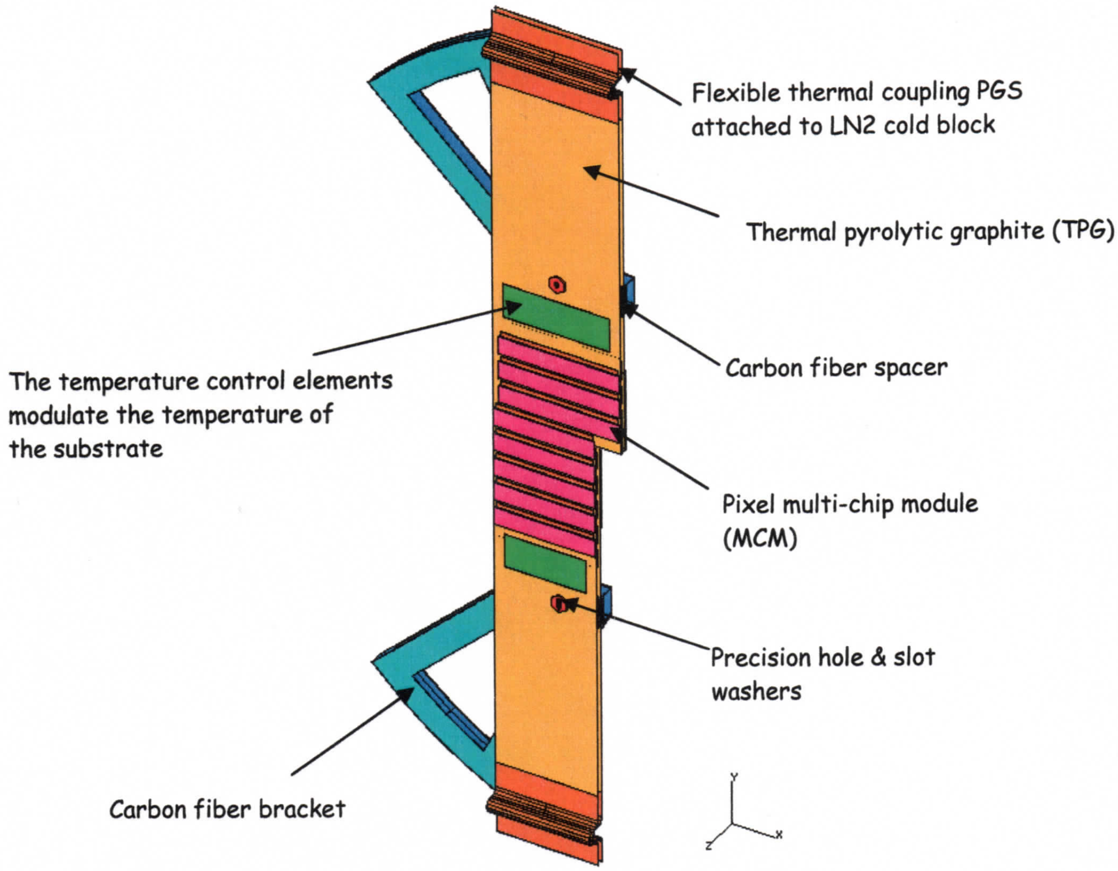

Figure 1. The BTeV pixel detector with Y-view measuring plane shown in front

The pixel multi-chip module (MCM) is made up of a stack of materials including the high density interconnect flex cable (HDI), the readout chips (ROC), the sensor modules which are bump-bonded to the ROCs. However, in this prototyping and testing phase, dummy modules, with the bump- bonded layer between the sensor and read out chips replaced by glue, were used. The stack of this dummy MCM is shown in Figure 2.

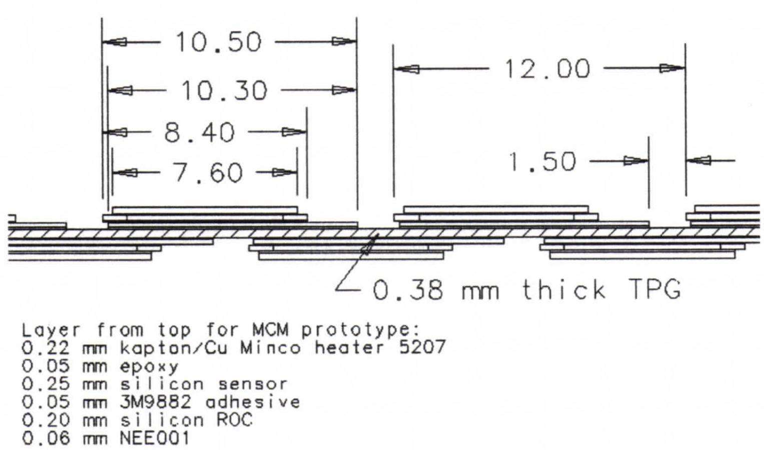

Figure 2. The lay-up of the dummy pixel multi-chip module (MCM)

II. Fabrication of prototype

Dummy silicon chips were made and cut with the DISCO dicing saw in Lab A. The sensor modules were from real mechanical grade wafers. The thickness of the sensor was 0.25 mm and that of ROC was 0.20 mm. The sensor piece was glued to a long piece of silicon using 3M9882 thermally conductive tape. This tape was chosen mainly because it had an equivalent modulus closer to that of bump-bond layer. A final dicing cut of 100 micron wide was then made on the long silicon piece to simulate a series of ROCs on the sensor. A set of 4, 5, 6 and 8-chip dummy MCM were all fabricated in this way. The layout of the MCM prototype was basically of the original design in which the HDI was glued to the top of sensor. To generate the heat load in these dummy silicon modules, Minco kapton heaters 5207 were used. These kapton heaters also simulated the HDIs since it was made also of kapton with copper circuitry enclosed. However, due to the size constraint of the MCM and the availability of heaters, these Minco heaters were smaller and did not match the size of the real HDIs that will be used in the experiment.

TPG substrates of 170 mm x 70 mm x 0.38 mm were used. After receiving the raw substrates from the vendor (GE Advanced Ceramics), a hole, a slot, and a notch for beam window were machined on the substrates at Fermilab. It should be noted that 170 mm will not be the full length of the final substrate which is about 400 mm long. Due to the handling considerations and the major interest of the study was focused on the central sensor area, this shorter version was therefore used for the prototyping. (For thermal testing, it was needed to provide a cold temperature boundary at this ends.) To improve the mechanical strength of the TPG pieces, perforated holes with a diameter of 0.15 mm arranged in a grid of 84x34 with center to center spacing at 2 mm were drilled with laser by a contracted workshop. The substrate was then encapsulated with parylene C. By doing so, a reinforcement was thus achieved as hundreds of parylene bonds connecting the top and bottom layers were formed. Some sort of fraying problems were encountered during the laser drilling process. It might be due to inherent delamination within the TPG pieces and local overheating of the laser energy. However, during multiple handling of these fragile pieces, some TPGs were fractured. Only 2 out of 6 pieces survived the full process and these were used for assembly as the X and Y-plane substrates. One of the fractured substrates was patched with carbon fiber prepreg. Together with another TPG with frayed-surface and a couple of carbon-fiber spacers, a station was formed by gluing the TPG pieces together so that a station prototype was available for the thermal sliding test.

Although Paraylene C was poor in adhesion, this adhesion could be significantly improved by plasma cleaning with oxygen as the reactant gas. Precision washers for the hole and slot pair were then glued with NEE001. A coordinate measuring machine (CMM) with optical camera was used to position these washers accurately. These substrates were then ready for the placement of the dummy modules.

An assembly fixture with 2 precision pins securing the TPG substrate in place was designed and fabricated. This design was shown in Figure 3. The end plates with the precision pins were designed to be adjustable. After several rounds of touch-probe measurements and adjustments, these end plates were fastened and the positioning accuracy was measured to be within 6 microns.

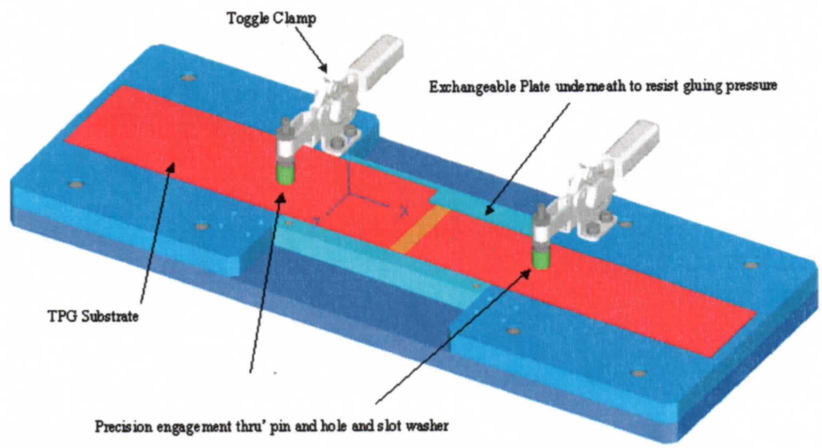

Figure 3. Tooling fixture for holding the substrate

The central plate was exchangeable and could be a flat plate or a finned plate depending on the MCM assembly progress. To start gluing the MCM on top of the substrate, a flush plate was used first. This flush plate provided a flat bed for supporting the TPG substrate evenly so that it would not get fractured when a pressure was applied on top during the gluing process. When done with this side, a finned plate was used instead. Due to the populated MCMs that had been already glued on the first side, the fin support was needed and they fit properly in between the gaps of the MCMs. As of the MCM placement, a module holding mechanism, which had 3 translational and 1 angular adjustment capabilities, was used. This scenario is as shown in Figure 4 and the placement was done correctly with the aid of CMM.

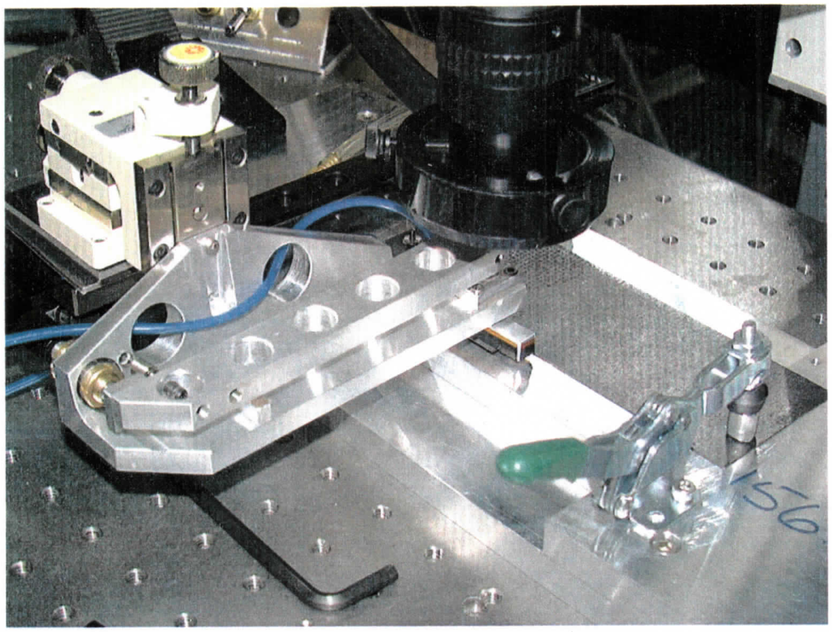

Figure 4. Assembling a multi-chip module (MCM) on TPG substrate

The assembly steps were detailed as follows:

- Engage the TPG substrate with the assembly fixture through the precision fittings
- Apply toggle clamps on washers and secure the TPG substrate.
- Apply 2.5 mil thick silicon glue NEE001 on the MCM with a simple gluing setup.
- Attach MCM on the vacuum holder of the module holding mechanism.
- Position the MCM with reference to the pin reference system.
- Apply 2 drops of UV glues at ends to secure the MCM in place temporarily.
- Repeat for the other MCMs on the same surface of TPG substrate.
- Remove the populated substrate carefully
- Replacethe flush plate with the finned plate for the other side of MCM placement.
- Position all MCMs as described previously.

Minco heaters were then glued on the top of MCMs. Due to the need of exposing the fiducial targets which were located at the corners of sensor, the smallest model 5702 was used. We used one heater on each MCM except for the 8-chip MCM which had 2 heaters. These heaters all came with pressure sensitive adhesive on the back and hence were glued directly on top of the MCMs.

Additional targets were glued on the substrate. The spatial positions of these targets would be used to understand the thermal displacement when the heaters were turned on. Resistance temperature detectors (RTD)s were also glued on the MCMs and the substrate for measuring the thermal profile. These 100-ohm RTDs had an allowable deviation of +/- 0.3C at 0C and +/-0.8C at -100C and thus were good enough to be used directly without calibration. The distribution of these targets and RTDs was shown in Figure 5 and Figure 6. All the wires of heaters and RTDs were clamped appropriately for strain relief purpose.

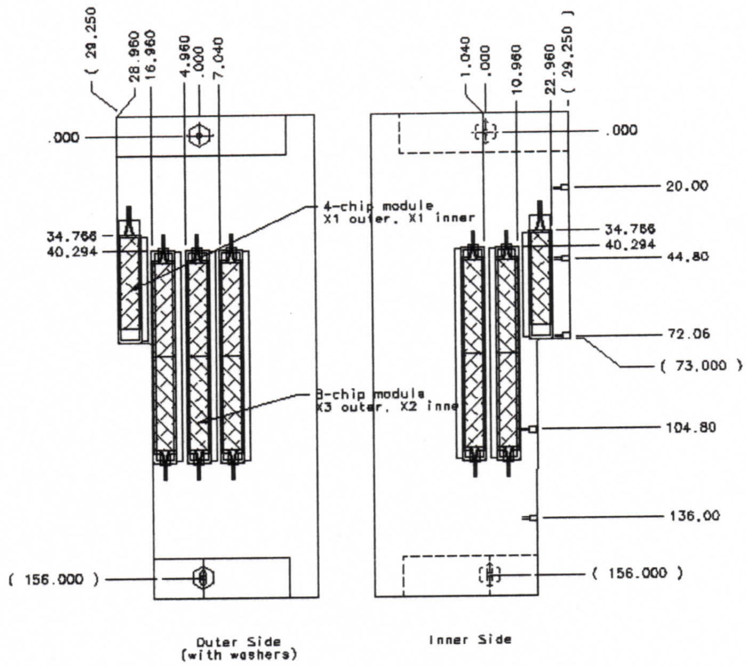

Figure 5. RTD mapping on X-view substrate

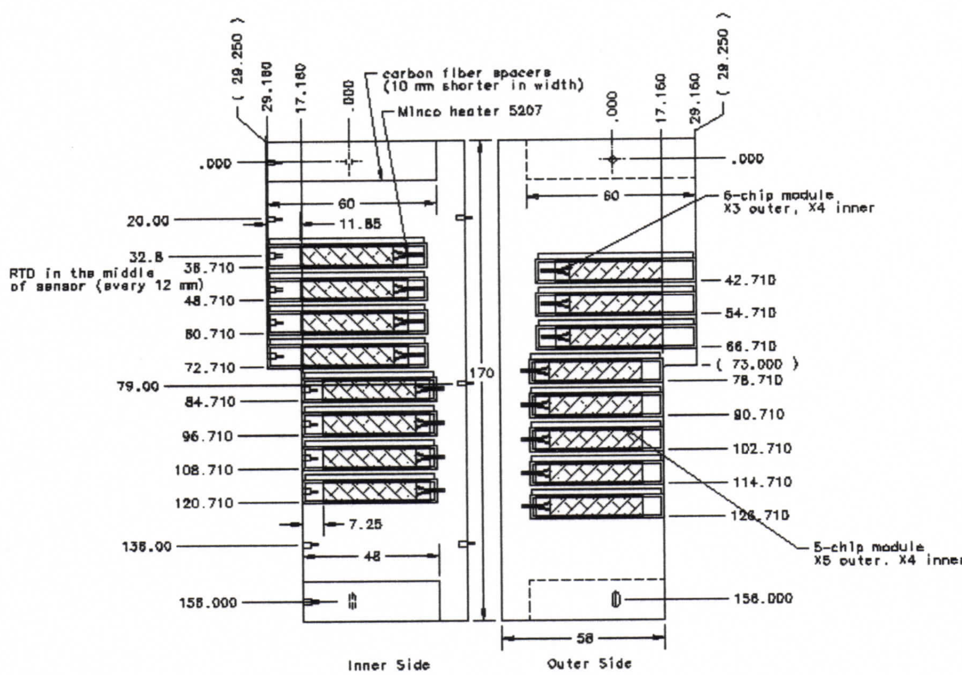

Figure 6 RTD mapping on Y-view substrate

The positioning accuracy was checked using another optical CMM - OGP. The largest deviation from the nominal position was found to be 81 microns. This large deviation was probably due to the use of the precision pin circumference, rather than a fine cross-hair target, for setting up the reference datum when measured by the optical camera. It should be noted that these deviations would not hurt the thermal displacement test as long as the actual amount of displacement of each point was monitored.

III. Fabrication of the test setup

A dry box was designed and made for the thermal test. Since the major interest of this test was the thermal displacement of the central sensor area within the precision fitting supports, a small dry box to accommodate the central portion of substrate would fit well on the movable OGP table. OGP was used because it had the best capability in focusing targets in Z direction automatically with a precision within 5 microns. This dry box was attached with two cold blocks at the ends for supporting and cooling the TPG substrate. Coolant like water glycol with 50/50 mixture ratio by volume was used and it ran through these cooling blocks. Dry nitrogen was needed to purge the box before and during the test to prevent any frost from setting on the substrate. This box was made of aluminum except the cover plate which was made of Plexiglass in order that the camera can see it through. This set up was shown in Figure 7. To confirm that the Plexiglass would not generate fake data, a validation check with camera seeing target with and without the Plexiglass was made and compared. The outcome was good and basically there were no difference.

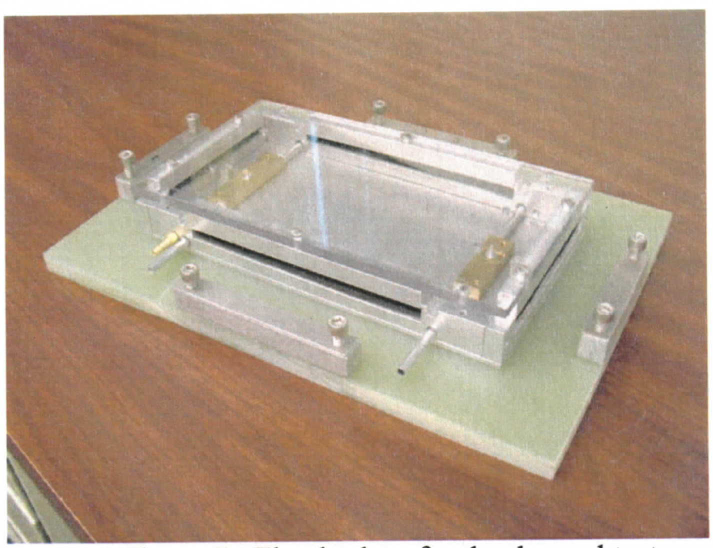

Figure 7. The dry box for the thermal test

A pair of precision pins of the size of 2 mm were glued on the cold blocks. One pin engaged with the precision-hole washer of the TPG substrate while the other engaged with the precision-slot washer that allowed the substrate to slide longitudinally when temperature changed. It should be noted that there was a major difference about this fitting in the actual design and the thermal test set up. In the actual design, since only a small amount of capturing force was needed to prevent the station from falling, an O-ring compressed slightly by a tiny screw was provided. This is shown in Figure 8 in which part of the whole station consisting of the X and Y-view substrates and carbon fiber spacer are compressed. However, in the thermal test, this set up could not be employed as the substrate alone was much thinner. In addition, the substrate needed a much tighter contact with the cold blocks (which were not in this location but at the ends in real operation) so that the temperature drop across the contact was small but it could not be provided by this tiny screw. This set up was modified slightly and the amount of tighter pressure was eventually provided by compressing some foam strips under the top cover instead.

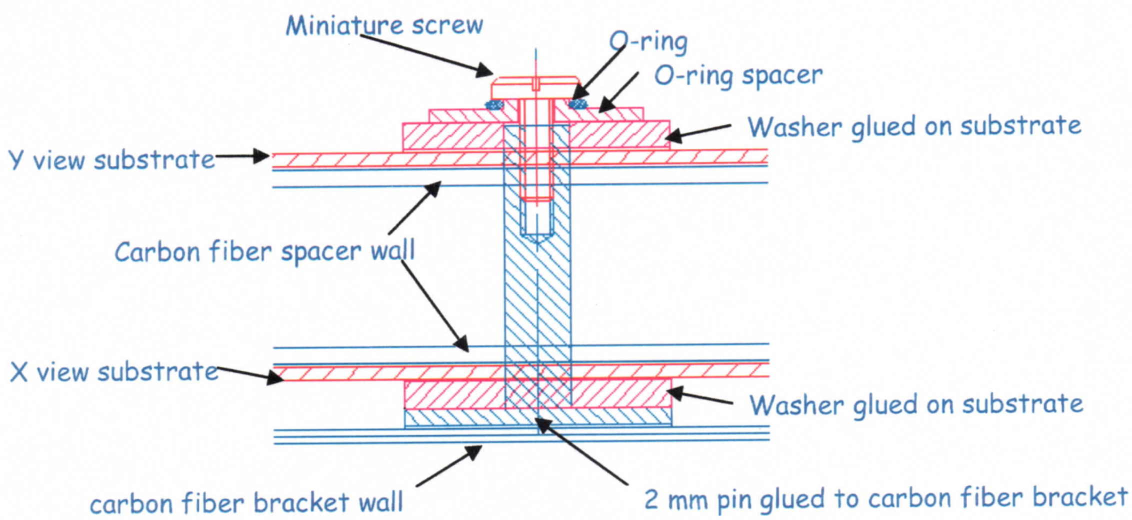

Figure 8. Precision fitting design

IV. Thermal sliding test of station prototype

Before the thermal tests on the substrates, the sliding capability of the station was check. As friction between the substrate and the support would be generated when the O-rings were compressed, this amount of compression needs to be understood as well. Based on the market availability, the O-ring with a nominal diameter 2 mm and thickness 0.4 mm was chosen. And the selected material was silicone as its flexibility could still be retained well even at low temperature like –60C and it was acceptable for vacuum uses. Six O-rings were compressed one by one with a Dillon force gauge and the displacements were recorded by an electronic dial gauge. The results were shown in Figure 9 from which it appeared that 2 lbs of capturing force would be generated if the O-ring was compressed to 0.3 mm.

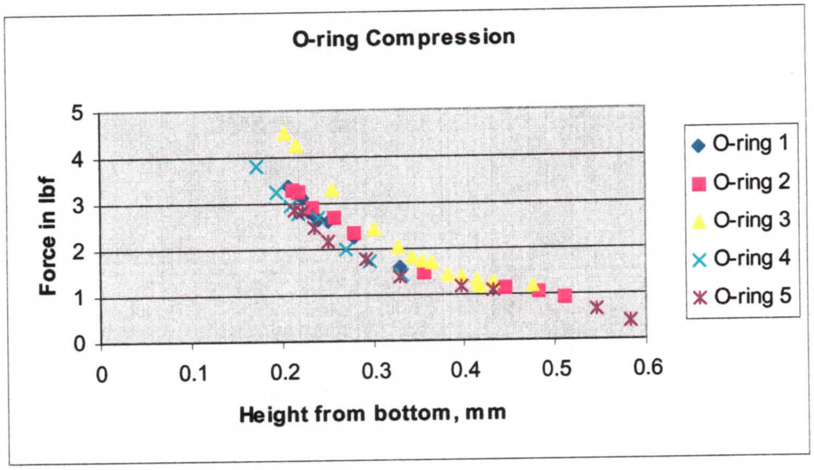

Figure 9. Results of compressing O-rings

As mentioned above, a bare station consisted of patched up substrates without any dummy MCM was used for this test. To facilitate and monitor this sliding test, precision washers and a series of targets were glued on the station. To provide the temperature change, a cold block support was provided. As temperature got colder, due to the negative and positive coefficient of thermal expansion (CTE) of the TPG substrate and the aluminum support, the substrate would elongate while the cold block would shrink. Therefore, the substrate might bow if friction was too high and the substrate could not slide relative to the support. (Aluminum support was used to amplify this phenomenon for inspection. In actual operation, this support would be made of nearly zero-CTE carbon fiber). This set up is shown in Figure 10 in which the fittings of the station were engaged with the pins extended from the cold block supports, and the whole set up was enclosed within a dry box being purged by dry nitrogen. One end of the aluminum cold blocks was glued while the other end was allowed free to slide. Two targets were glued at the ends of the cold block for displacement check uses.

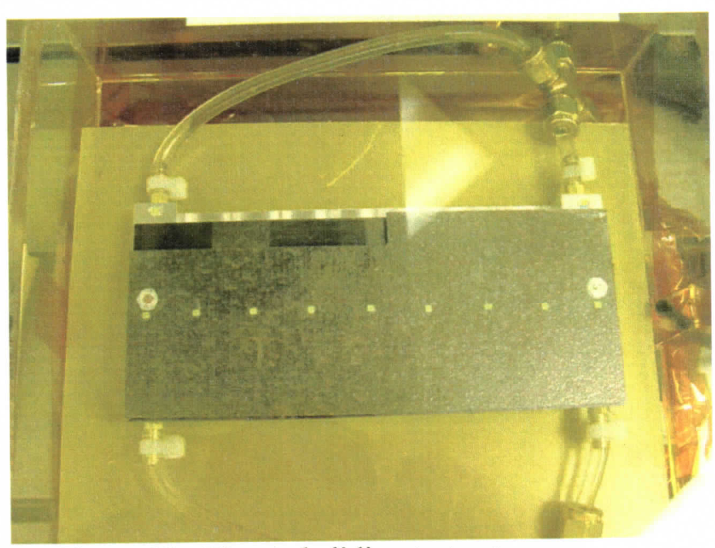

Figure 10. Thermal sliding test set up

This thermal sliding test was done on a CMM machine. For a temperature drop of 39C from 20C to –19C at the cold block, it was found that the aluminum support shrunk 0.1289 mm while the TPG piece expanded by 0.0117mm. No apparent bowing was observed in this test. The sliding performance was as good as expected.

V. Thermal displacement test of X-plane substrate

Before the thermal testing, a small piece of TPG glued with MCM and Minco heater was made and tested in order to understand the temperature deviation on different surfaces. This piece of TPG was then glued to the aluminum cold block that had been used for the thermal sliding test. RTDs were glued to the surfaces of Minco heater, silicon, TPG and aluminum cold block. Temperatures were recorded without power, with half and full power inputs based on the expected power density with the real operating detector modules. . This set up is shown in Figure 11, and the results are shown in Table 1. There was about 4 C in difference when comparing the temperatures on sensor silicon and TPG substrate at full power level.

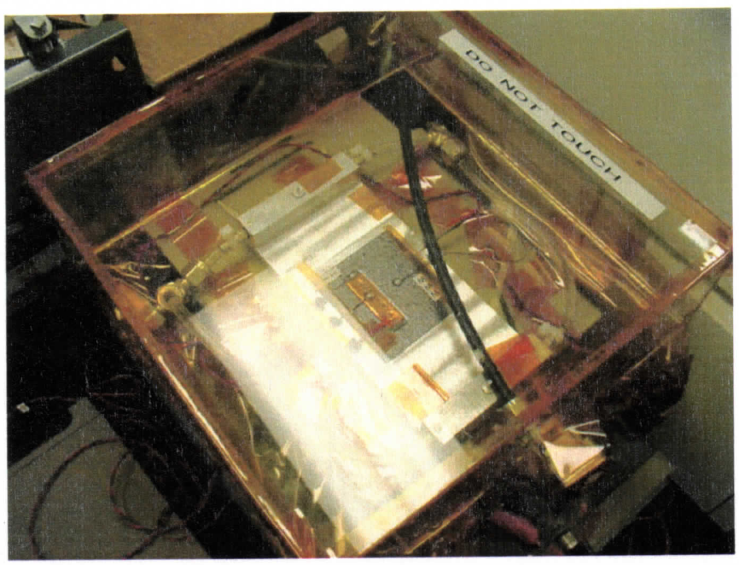

Figure 11. Temperature distribution test set up

Power, W	Temperatures, C			
	Aluminum	TPG	Silicon	Heater
0.00	-18.5	-17.9	-17.1	-17.1
1.84	-16.1	-14.7	-11.6	-2.9
2.88	-14.9	-13.1	-9.0	4.7

Table 1. Temperature results as recorded by RTDs on different surfaces

The thermal displacement test was done on the OGP which had a stationary optical camera on top with a movable table. The advantage of using OGP was the speed. With an aid of a program, it moved and focused on targets quickly. However, a proper strain relief on the plumbing lines was needed otherwise the substrate might be displaced due to the movement of table. Before the test was conducted, a preliminary run with the chiller system was made to confirm the desirable temperature was obtainable without any coolant leakage. After the following improvements were made, the chiller could then deliver a temperature about –30C at the cold blocks when the 21 W heat load was turned on.

- Adopted a powerful chiller Neslab CB80 that could provide temperature down to -80C;
- Used thermal grease to reduce the temperature drop across the substrate and the cold block;
- Placed extra foam materials between the top cover and the cold block to improve the thermal contact. It was needed as the capturing force provided by the tiny screw at the precision pin was not enough to keep the substrate in good contact with the cold block;
- Changed the coolant to Dynalene HC-50 which is a safe water-based coolant and has much favorable heat transfer properties like freezing point, viscosity, heat capacity, and heat conduction.

The thermal data of the substrate at room temperature, at chiller temperature -35C without, and with the heaters on, as recorded by the RTDs were as shown in Figure 12 and Table 2. It was found that the temperature ranges over the sensor area were about 0C, 4C and 6C correspondingly. (Numbers in black are temperature readings while numbers in red are locations.)

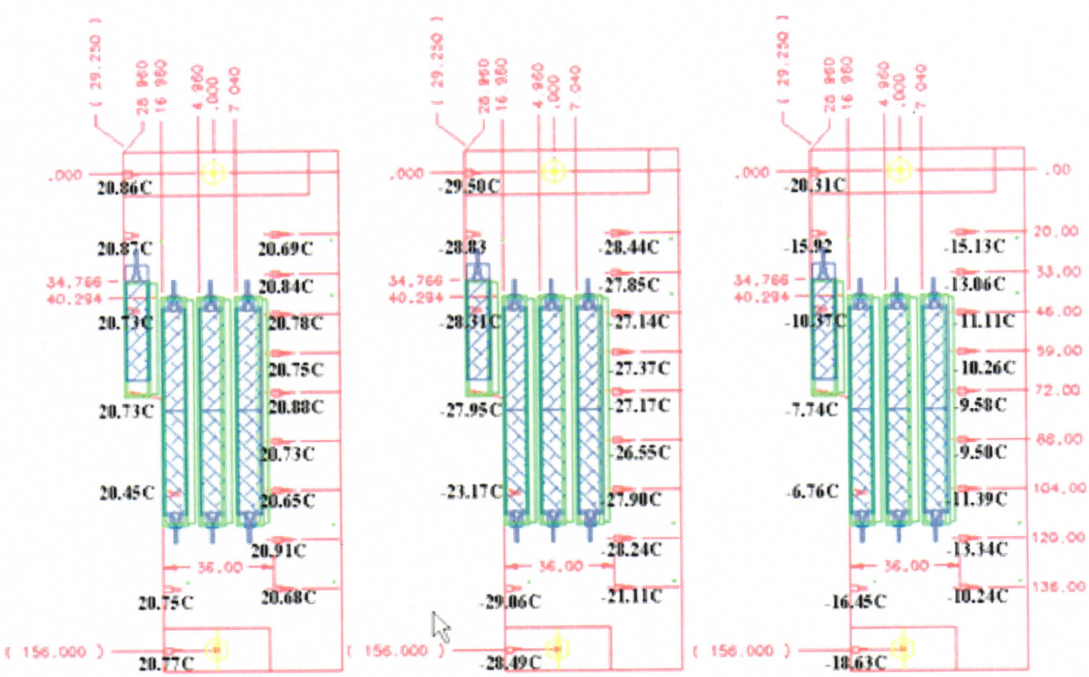

Figure 12. Temperature recorded on X-plane substrate

Thermal Condition	Temperatures Range over Sensor Area, C

Room Temperature	0
Chilled with Heaters Off	4
Chilled with Heaters On	6

Table 2. Temperature results as recorded by RTDs on different surfaces

Some FEAs were run to simulate the testing conditions. The material properties used in the model were listed in Table 3. It was found that both the radiation and convection heat gains from the surrounding were small at about 5% of the heaters load in the preliminary runs. These additional heat loads were thus disregarded in the final run and the final temperature distribution with a heat load 21W is shown in Figure 13.

	Heater	Silicon	Glue	TPG
Elastic Modules *E* (MPa)	2600	110e3	0.76	83e3
Poison's Ratio	0.35	0.30	0.45	0.20
Conductivity *k* (w/mm-C)	0.1564e-3	0.141	0.26e-3	Table II
CTE (1/C)	27e-6	2.6e-6	100e-6	-1e-6

Thermal Conductivity of TPG

T (C)	-203	-193	-183	-173	-123	-73	-23	0	26.8
k (w/mm-C)	2.92	3.43	3.78	3.89	3.62	2.60	1.96	1.78	1.60

Table 3. Material Properties Used in the Model

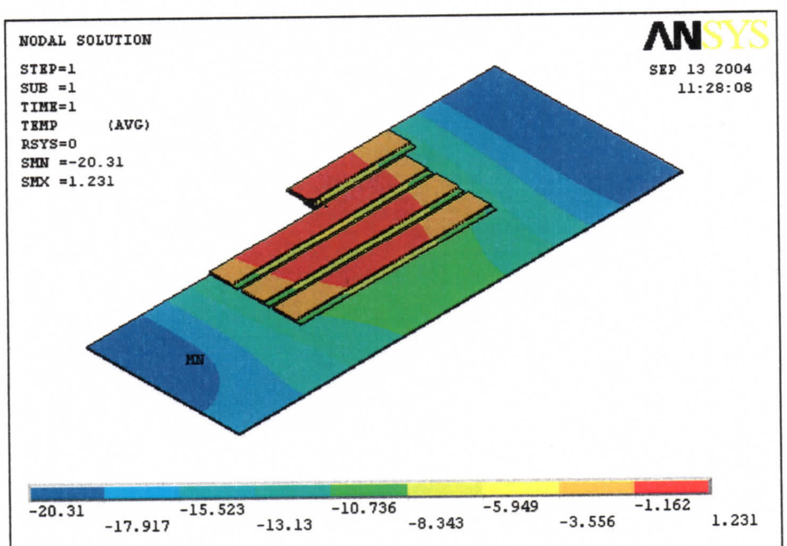

Fig.2 Temperature Distribution of Test Model

Figure 13. FEA Temperature Distribution of X-view Substrate

A comparison of the measured data against the results of FEA in case that the heaters were turned on is shown in Figure 14. Two sections were compared. It can be seen that they agree with each other very well.

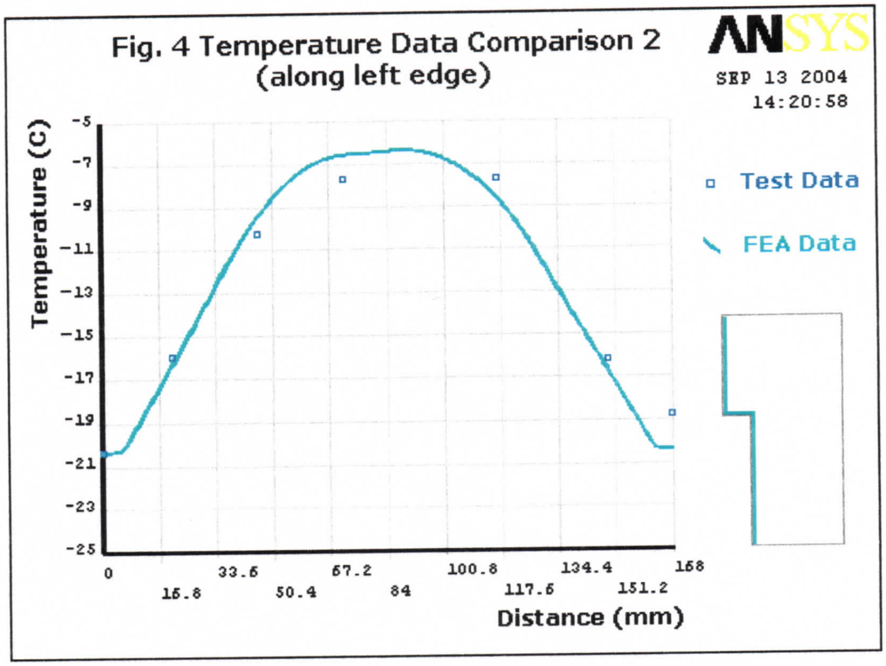

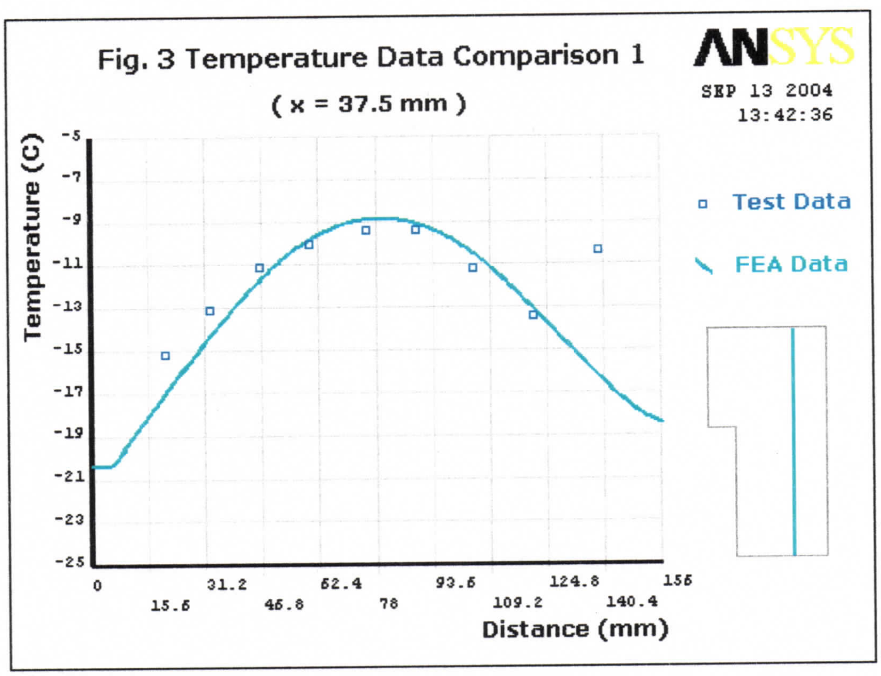

Figure 14. Comparison of Measured Data against FEA Results for X-view Substrate

To eliminate any possible relative displacement of the substrate with respect to the stationary pin due to the tiny clearance between the pin and the hole, the substrate was spot glued at the pin while the other end was still let free. The displacement results were shown in Figures 15. It was found that the in-plane displacement of the targets was only in few microns even for a temperature change of 56C from +21C to -35C. The out-of-plane displacements appeared larger; however, it should be noted that the in-plane measurement deviation was just about three microns while the out-of-plane measurement deviation was 14 microns due to the focusing uncertainty error. For reference, a plot showing the distorted profile at two different sections is shown in Figure 16. (Numbers in red are locations, same for the following figures.)

		Δx, mm	Δy, mm	Δz, mm
Targets on substrate	T1	-0.005	-0.003	0.035
	T2	-0.005	-0.003	0.031
	T3	-0.001	-0.002	0.021
	T4	-0.001	-0.002	0.025
	T5	-0.006	0.001	0.022
	T6	-0.001	0.004	0.035
Targets at silicon corners	S1	0.000	0.000	0.018
	S2	0.001	-0.001	0.016
	S3	-0.004	0.001	0.012
	S4	-0.004	0.000	0.015
	S5	0.000	-0.001	0.015
	S6	-0.004	0.001	0.011
	S7	-0.001	-0.001	0.017
	S8	-0.004	0.001	0.015
	S9	0.000	0.001	0.008
	S10	-0.004	0.002	0.013
	S11	0.000	0.001	0.008
	S12	-0.004	0.002	0.019
	S13	-0.001	0.002	0.000
	S14	-0.002	0.003	0.021

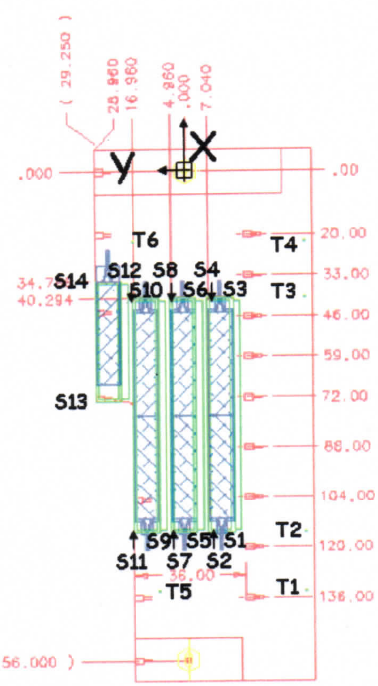

Figure 15. Displacement Results of X-view Substrate

Displacement Results
from +21C to –35C with heaters on

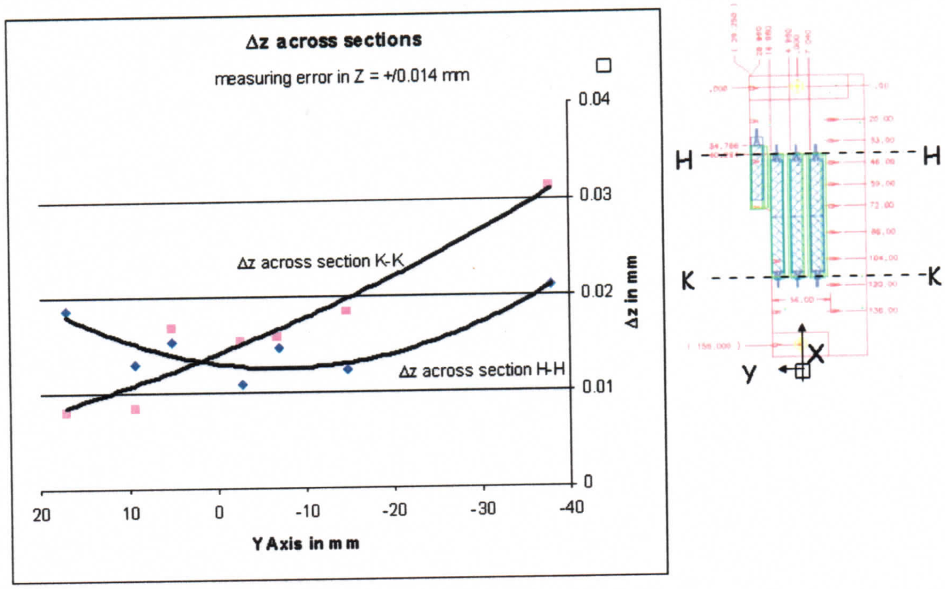

Figure 16. Distorted Profiles of X-view Substrates in two different Sections

A power failure scenario of one of the silicon module was also simulated. For example, the 2.4 W supposedly generated from one of the 8-chip modules was lost. The resultant temperature distribution is shown in Figure 17 in which all the RTDs are 0.5C to 2.3C colder than the nominal value and the changes are shown in the Figure 18. The transient response of this power loss at the hottest spot is shown in Figure 19 in which the temperature of the substrate was found to stabilize in less than 1 minute after the power loss of one module

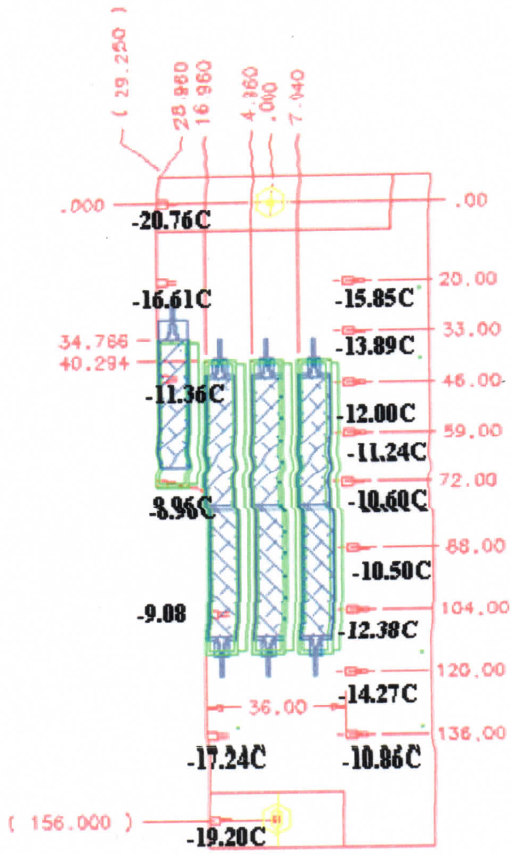

Figure 17. Temperature Results when one 8-Chip Module was turned off

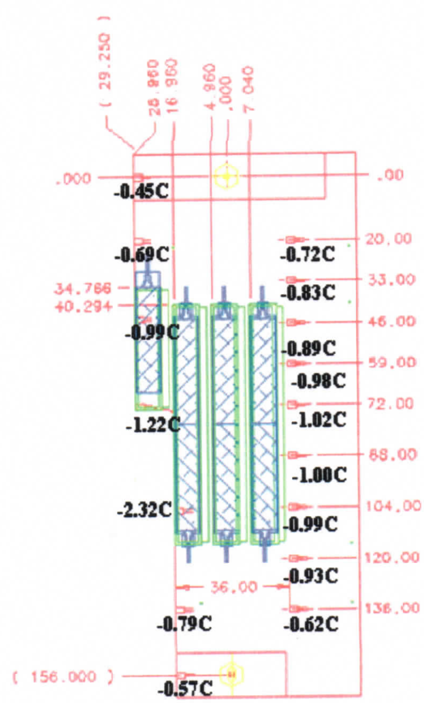

Figure 18. Temperature Changes when one Chip was powered off

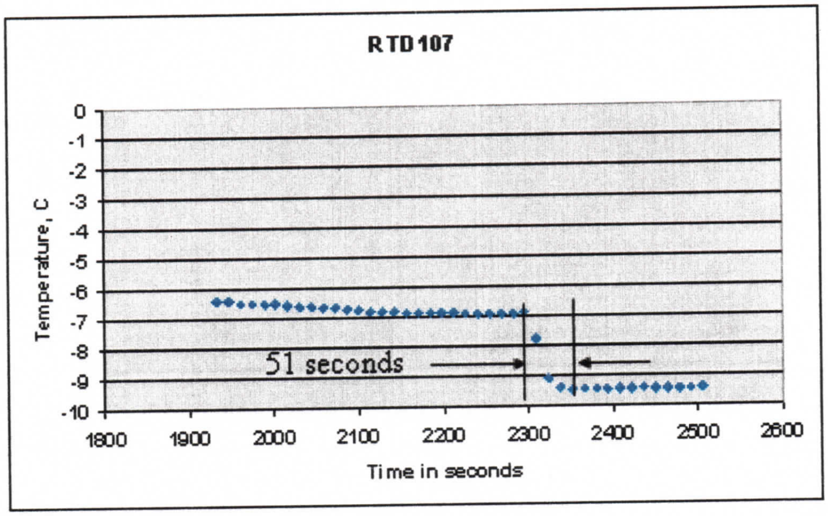

Figure 19. The Transient Response when the 8-Chip Module was turned off

VI. Thermal displacement test of Y-plane substrate

A similar test box made of PVC instead of aluminum was used to hold the Y-plane substrate. As the heat load was higher for this substrate, the chiller was required to provide coolant at -50C to conduct the test. As the coolant Dynalene had a freezing temperature at -55C, this made the chiller system running at the limit.

Due to the availability and the strain relief problem of the cooling lines on the movable table of OGP, this test was conducted on the Brown & Sharp CMM which was equipped with a X10 optical lens. The time consumed to make a clear focus at the target was longer, but it eliminated the strain relief issue of the movable cooling line.

This test had some other problems in the early runs when it was tested on the OGP. After five thermal cycles were done, some silicon modules were found partially delaminated from the substrate. These silicon dummy modules were then completely removed, cleaned and then re-glued. Using dental floss to remove the adhesive NEE001 layer was found to be very effective.

Test was resumed on the Brown & Sharp. More problems were found after 3 cycles were run. Due to the deterioration of the quality of thermal grease after months of uses, the substrate was hold rigidly and was not allow to slide when in the cold state. This in turn made the substrate bow up more than 1 mm at the center. Fortunately, this upward bow did not break the delicate substrate. But it did interrupt the test and the thermal cycling effect on the displacement check could not be continued. The substrate was removed for replacing the thermal grease completely.

Another delamination check was done when the apparatus was reset. A 2-mil shim was used to inspect if there was any gap between the silicon and substrate. Some voids were found along the perimeter of the silicon. Without removing the silicon, these voids were filled with thermal grease and test was resumed for another 2 more cycles. However, it was verified that these additional sets of displacement results could not be used to compare with those of previous ones. It is thus only the results of the first 3 cycles are reported.

The typical temperature profiles of the measurement are as shown in Figures 20, 21 and 22. A FEA temperature plot, and the temperature comparison of the sections MM and NN to the FEA are shown in Figure 23, 24 and 25.

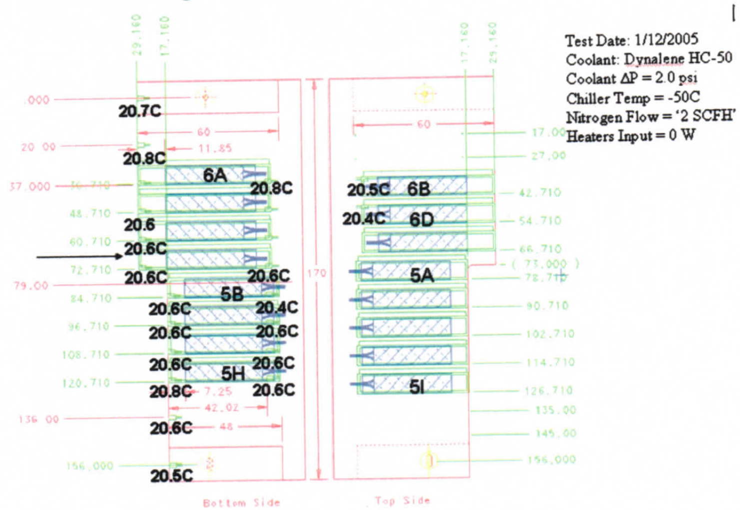

Figure 20. RTD Temperature Results at room temperature on the Y-view Substrate

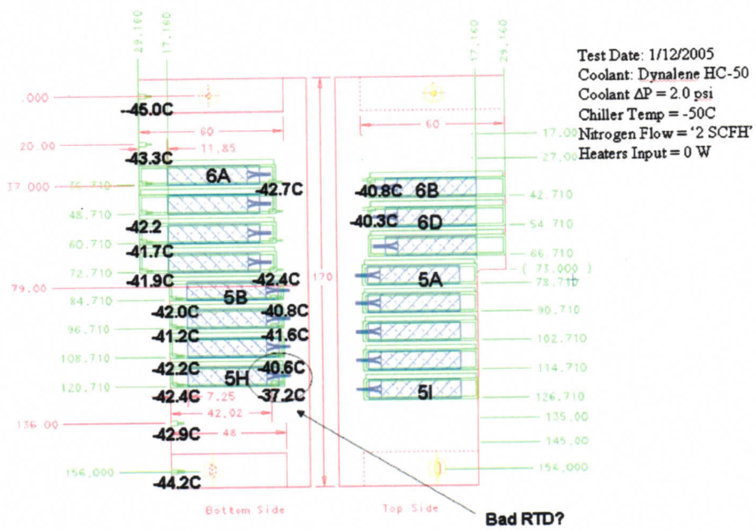

Figure 21. RTD Temperature Results at chilled temperature on the Y-view Substrate

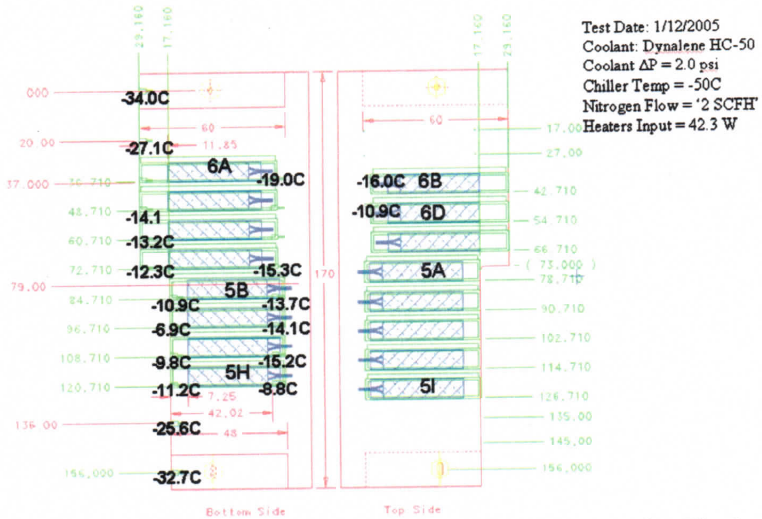

Figure 22. RTD Temperature Results with the heaters on on the Y-view Substrate

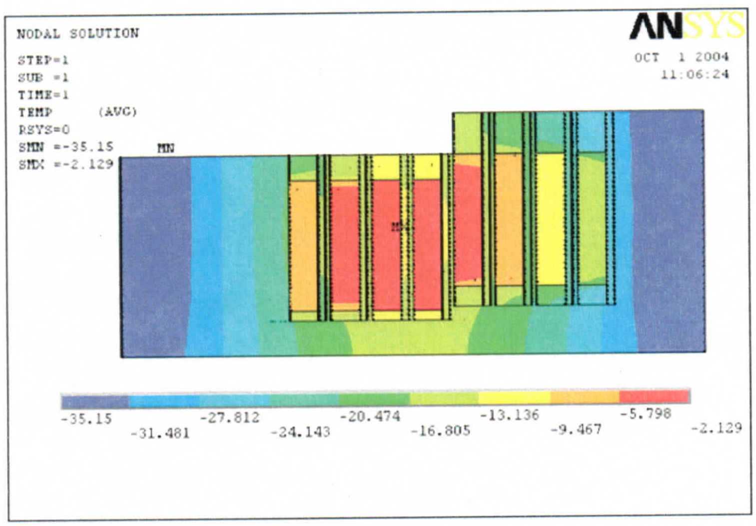

Figure 23. FEA Temperature Results with heaters on on the Y-view Substrate

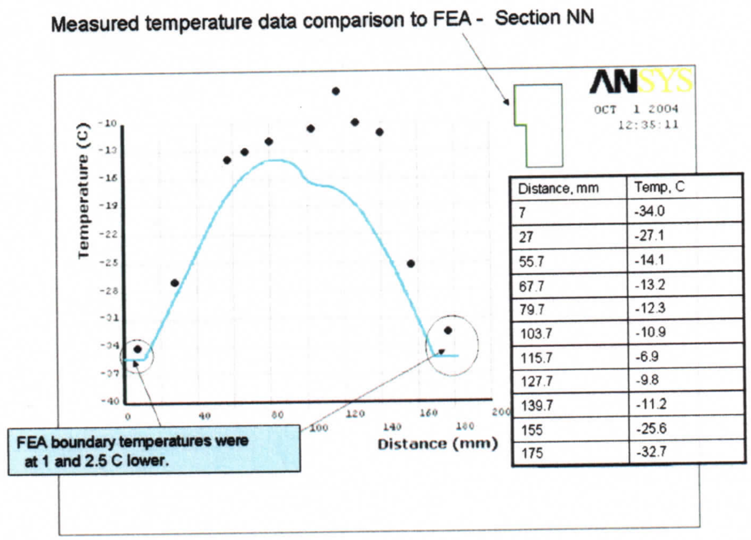

Distance, mm	Temp, C
7	-34.0
27	-27.1
55.7	-14.1
67.7	-13.2
79.7	-12.3
103.7	-10.9
115.7	-6.9
127.7	-9.8
139.7	-11.2
155	-25.6
175	-32.7

Figure 24. Temperature Results Comparison on Section NN on the Y-view Substrate

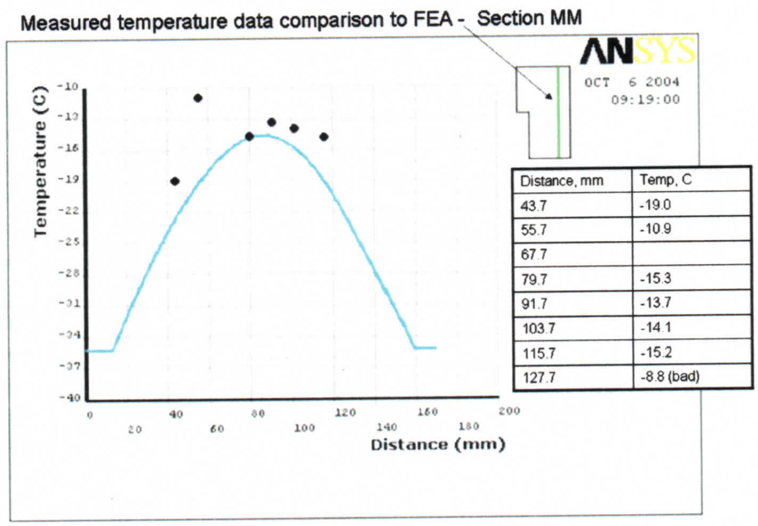

Distance, mm	Temp, C
43.7	-19.0
55.7	-10.9
67.7	
79.7	-15.3
91.7	-13.7
103.7	-14.1
115.7	-15.2
127.7	-8.8 (bad)

Figure 25. Temperature Results Comparison on Section MM on the Y-view Substrate

The displacement results are shown in Table 4. This was done by comparing data sets between room temperature and chilled with heaters on. An average of the three measurements is reported and it can be seen that the in-plane displacement is while the out-of-plane is slightly larger. The measuring errors for this Y-view substrate are basically the same as reported for the X-view substrate, it is about 3 microns for the in-plane and 16 microns for the out-of-plane measurements. To see the thermal cycling effect, all the three heaters-on data sets are compared. This result is shown in Table 5 in which the measuring errors for each point in terms of the standard deviation of x, y and z are shown in the last three columns. The averages of these standard deviations were computed in the bottom of the table and they are very small. Since the displacement amounts were very small, and these standard deviations were comparable to the actual displacements, one could conclude that the substrate basically returned to the same deformed shape when the heaters were turned on. A comparison of these measured displacement data against FEA were plotted in Figures 26 and 27 in which they show the in-plane displacements dx and dy are matched reasonably well while the out-of-plane displacement dZ is a little bit farther away due to the focusing uncertainty error.

		Average of 3 cycles			std dev		
FEATURE	Y	dX	dY	dZ	dX	dY	dZ
GF_1	16.966	0.000	-0.001	-0.010	0.001	0.001	0.005
GF_2	25.767	0.000	-0.001	-0.007	0.001	0.000	0.008
GF_3	134.955	0.000	0.006	0.005	0.001	0.003	0.003
GF_4	144.271	-0.001	0.005	0.003	0.001	0.004	0.010
GF_5	144.759	0.005	0.006	0.000	0.001	0.006	0.009
GF_6	134.953	0.005	0.005	-0.009	0.000	0.006	0.002
GF_7	25.897	0.005	0.000	0.004	0.003	0.003	0.013
GF_8	16.967	0.003	-0.002	0.044	0.008	0.001	0.066
5I1	126.690	0.003	0.002	-0.005	0.000	0.008	0.011
5I2	118.870	0.004	0.002	-0.002	0.000	0.008	0.008
5I3	126.663	0.003	0.003	-0.003	0.001	0.004	0.008
5I4	118.843	0.003	0.004	0.005	0.000	0.004	0.011
5G1	114.693	0.003	0.003	-0.004	0.001	0.008	0.010
5G2	106.874	0.004	0.004	0.001	0.000	0.008	0.020
5G3	114.677	0.003	0.002	0.000	0.000	0.004	0.017
5G4	106.858	0.003	0.003	0.008	0.000	0.004	0.020
5E_1	102.691	0.002	0.003	0.005	0.000	0.008	0.028
5E_2	94.873	0.003	0.003	0.010	0.001	0.007	0.022
5E_3	102.673	0.001	0.000	0.012	0.000	0.004	0.022
5E_4	94.854	0.001	0.001	0.012	0.000	0.004	0.026
5C1	90.893	0.003	0.001	0.011	0.001	0.007	0.019
5C2	83.073	0.004	0.001	0.009	0.001	0.008	0.020
5C3	90.712	0.002	-0.001	0.007	0.000	0.004	0.026
5C4	82.892	0.002	0.000	0.002	0.001	0.004	0.019
5A1	79.018	0.003	0.000	0.013	0.001	0.008	0.016
5A2	71.199	0.003	0.000	0.006	0.001	0.007	0.014
5A3	78.832	0.002	0.000	0.010	0.000	0.004	0.018
5A4	71.012	0.002	0.000	-0.002	0.001	0.004	0.020
6F1	66.694	0.000	-0.001	-0.003	0.001	0.006	0.022
6F2	58.873	0.000	0.000	-0.002	0.002	0.006	0.012
6F3	66.767	-0.002	-0.001	-0.001	0.000	0.003	0.017
6F4	58.946	-0.002	0.000	0.005	0.002	0.002	0.024
6D1	54.693	-0.001	-0.002	0.003	0.002	0.008	0.016
6D2	46.876	-0.001	-0.001	0.002	0.002	0.004	0.011
6D3	54.654	-0.002	-0.002	-0.002	0.001	0.002	0.012
6D4	46.834	-0.002	-0.002	-0.010	0.001	0.002	0.013
6B1	42.691	0.000	-0.003	0.006	0.003	0.010	0.005
6B2	34.871	0.000	-0.002	0.014	0.002	0.006	0.009
6B3	42.648	0.000	-0.004	-0.013	0.001	0.001	0.009
6B4	34.828	0.000	-0.003	-0.010	0.001	0.001	0.004

	Average of standard deviation:			0.001	0.005	0.016

Table 4. Displacement Results on the Y-view Substrate

avg of 3 cycles				std dev		
FEATURE	x	y	z	x	y	z
GF_1	-15.793	16.964	0.019	0.000	0.000	0.003
GF_2	-16.028	25.766	0.031	0.001	0.000	0.002
GF_3	-15.793	134.962	0.271	0.000	0.002	0.003
GF_4	-15.340	144.277	-0.049	0.001	0.003	0.003
GF_5	29.157	144.769	-0.171	0.001	0.004	0.003
GF_6	30.047	134.961	0.021	0.001	0.004	0.002
GF_7	26.968	25.899	-0.015	0.001	0.001	0.005
GF_8	27.253	16.968	-0.005	0.006	0.000	0.062
5I1	30.031	126.698	0.756	0.001	0.004	0.007
5I2	30.186	118.877	0.828	0.001	0.004	0.007
5I3	-17.251	126.668	0.622	0.001	0.002	0.008
5I4	-17.247	118.849	0.699	0.000	0.002	0.008
5G1	30.030	114.702	0.819	0.000	0.004	0.005
5G2	30.182	106.882	0.871	0.000	0.005	0.006
5G3	-17.251	114.684	0.646	0.000	0.002	0.004
5G4	-17.250	106.865	0.727	0.000	0.002	0.008
5E_1	30.038	102.699	0.805	0.001	0.004	0.012
5E_2	30.191	94.880	0.940	0.001	0.004	0.012
5E_3	-17.245	102.676	0.747	0.000	0.002	0.009
5E_4	-17.242	94.858	0.873	0.001	0.002	0.002
5C1	30.385	90.899	0.741	0.000	0.004	0.010
5C2	30.565	83.079	0.736	0.001	0.004	0.008
5C3	-16.897	90.715	0.892	0.001	0.002	0.011
5C4	-16.867	82.896	0.905	0.001	0.002	0.003
5A1	30.322	79.023	0.554	0.000	0.004	0.009
5A2	30.503	71.204	0.632	0.001	0.004	0.011
5A3	-16.960	78.835	0.768	0.001	0.002	0.005
5A4	-16.929	71.015	0.833	0.000	0.002	0.011
6F1	27.341	66.698	0.717	0.001	0.003	0.011
6F2	27.482	58.877	0.678	0.001	0.003	0.010
6F3	-29.142	66.769	0.652	0.000	0.001	0.003
6F4	-29.152	58.948	0.620	0.001	0.001	0.008
6D1	27.243	54.697	0.646	0.001	0.003	0.007
6D2	27.398	46.878	0.649	0.000	0.003	0.006
6D3	-29.242	54.654	0.603	0.000	0.001	0.006
6D4	-29.237	46.835	0.592	0.000	0.001	0.004
6B1	27.247	42.694	0.546	0.001	0.005	0.002
6B2	27.403	34.873	0.546	0.001	0.002	0.005
6B3	-29.238	42.647	0.515	0.001	0.000	0.003
6B4	-29.232	34.828	0.514	0.001	0.000	0.001
	Average of standard deviation:			0.001	0.002	0.008

Table 5. Thermal cycling Results on the Y-view Substrate

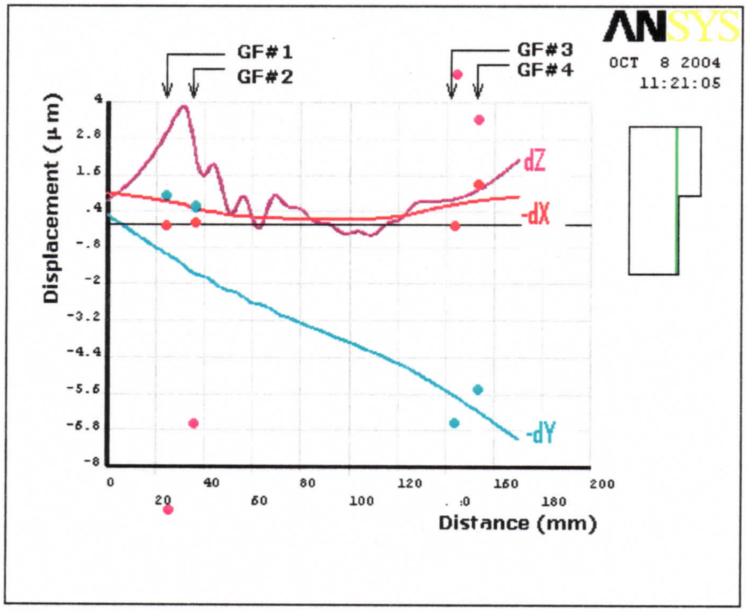

Figure 26. Displacement Results Comparison for Section NN on the Y-view Substrate

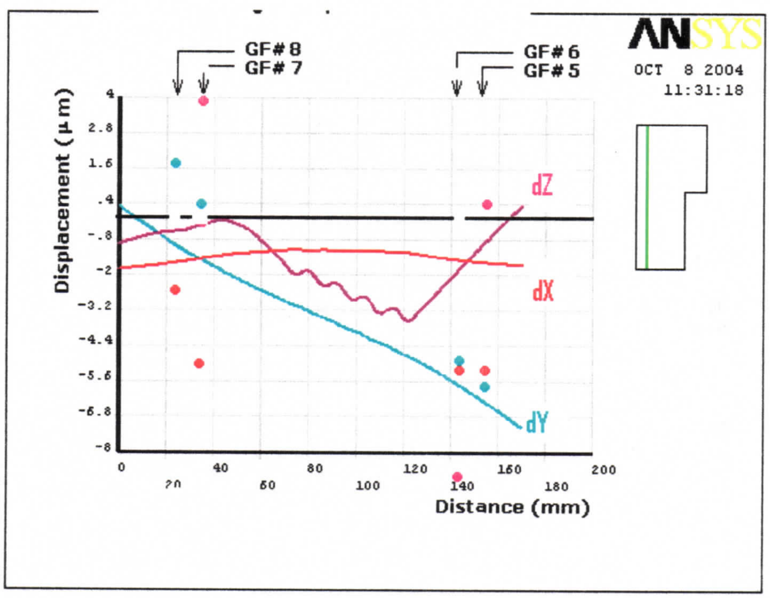

Figure 27. Displacement Results Comparison for Section MM on the Y-view Substrate

VII. Conclusions

A complete run down of the prototyping and testing of the substrates was addressed. It was found this substrate development was feasible and the testing displacements were small. No major alarm was observed in this TPG substrate development and testing.